International Journal of Scientific Engineering and Science
Volume 4, Issue 9, pp. 60-66, 2020. ISSN (Online): 2456-7361

Modified Computational Approach to Thermal Resistivity and Thermal Conductivity to Enhance Result Repeatability and Accuracy

Collins C. Chiemeke
Physics Department, Federal University Otuoke, Bayelsa State, Nigeria
E-Mail: chiemekecc @ fuotuoke.edu.ng Mobile Phone +2348035780638 or +2348078907930

***Abstract*— *Thermal resistivity or conductivity is a measure of the ability of soil material to conduct or dissipate heat from the source to the environment. Different soil types are characterized with their diverse thermal resistivity and conductivity values, which also indicate its ability to dissipate heat generated by a pipeline or electrical cable. The ranges of thermal resistivity values are so close that, slight change in temperature with the conventional method of computational could cause the result to differ appreciably, which could lead to wrong interpretation. Hence, this research work is aimed at developing a new computational approach that will improve thermal resistivity result accuracy and repeatability. The method employed in data acquisition involves measuring temperature changes due to heat source as a function of time. The new computational approach results revealed wide differences that exist between range of thermal resistivities determined through stepwise technique, of which if any of these individual value is adopted as the actual thermal resistivity result, as it is always the case in conventional approach, it could lead to erroneous result. The result also exposed the fact that the thermal resistivity and conductivity results determined with modified computational approach showed a high level of consistency and accuracy that was conveniently tied to the soil lithological composition at that depth. The conventional method of computation registered a high level of disparity and inconsistency in values, that could not be tied to any lithological composition, or effectively be used to for soil classification, for safety purpose. The first two digits in thermal resistivity values, by which thermal resistivity is mainly reported, showed a high level of uniformity at both survey points, which are clear indication of high repeatability in the thermal resistivity results. The statistical analysis carried out on the thermal resistivity results determined with modified computational approach had the least standard deviation from the mean compared to the conventional techniques. It is a clearly evident that the modified computational approach is a better and effective technique for obtaining more accurate and reliable thermal resistivity results with high level of repeatability.*

***Keywords*—*Computational Approach, Thermal Resistivity, Thermal conductivity, accuracy, repeatability.*

I. INTRODUCTION

One of the major reasons that necessitated the modification of the conventional computational technique is gross variation of the thermal resistivity values determined at the same point, same depth, and with same instrument. Part of the reason could be attributed with ambient soil temperature when the thermal resistivity is determined at the near surface [5] or variation of soil water content [4]. However, this research is geared toward mitigating the effect of these factors and enhances the repeatability and accuracy of the determined thermal resistivity in the face of changing ambient soil temperature and soil water content. Thermal resistivity or conductivity is a measure of the ability of soil material to resist or dissipate heat from a heat source to the environment. Thermal Resistivity σ, is mathematically expressed as:

$$\sigma = \frac{4\pi}{Q}\left[\frac{T_2 - T_1}{ln\left(\frac{t_2}{t_1}\right)}\right] \quad (1)$$

Where
$\sigma = Soil\ Thermal\ Resistivity\ (Km/W)$
$Q = Heat\ Input\ in\ W/m$
$T_1 = Temperature\ at\ time\ t_1$
$T_2 = Temperature\ at\ time\ t_2$
The unit (Km/W), represent "Kelvin, meter per Watt".
The inverse of thermal resistivity is referred to as thermal conductivity λ, mathematical express as:

$$\lambda = \frac{Q}{4\pi}\left[\frac{ln\left(\frac{t_2}{t_1}\right)}{T_2 - T_1}\right] \quad (2)$$

Where
$\lambda = Soil\ Thermal\ Conductivity\ (W/Km)$
All the parameters in equation 2 retain their usual meaning.

The range of thermal resistivity values for quartz and soil materials is between 0.1 ^{o}Cm/W to 0.4 oCm/W, and 1.7 ^{o}Cm/W to 40 ^{o}Cm/W for organic material, water and air, and the optimum safety standard for buried pipelines and cables is 0.9 ^{o}Cm/W, after [12]. This show that the range of thermal resistivity which is inverse of conductivity for earth material are so close that any slight change in temperature with time at the coordinate points where the slope of thermal resistivity is determined could result in a drastic change in the thermal resistivity value, that could lead to wrong interpretation and recommendation which could ultimately result in severe damage in infrastructure, when using conventional method of computation. In a bid to improve on the result accuracy and repeatability, a modified computational approach that is more robust and accurate was developed. The method took into cognizance the possibility of making use of average multiple slopes, compared to the previous single slope computational techniques, with obvious discrepancies at the boundaries of the coordinate points. Considering previous research, [10] stated that "Soils containing a high percentage of quartz will have a lower thermal resistivity than those containing a high

International Journal of Scientific Engineering and Science
Volume 4, Issue 9, pp. 60-66, 2020. ISSN (Online): 2456-7361

percentage of mica, all other things being equal". Areas of hot weather shall be given special attention as drying of subsurface soils can cause the resistance to heat transfer to increase [9].

II. Geology of the Area

The Formation of the present Niger Delta started during Early Paleocene as a result of the built up of fine grained sediments eroded and transported to the area by the River Niger and its tributaries. The regional geology of the Niger Delta consists of three lithostratigraphic units; Akata, Agbada and Benin Formations, overlain by various types of Quaternary Deposits [8], [7], [1]. These Quaternary Sediments, according to [11] are largely alluvial and hydromorphic soils and lacustrine sediments of Pleistocene age.

III. Location of Study Area

The study area is located at Yenagoa, Bayelsa State, Nigeria, with an average elevation of 15 m, above sea level, after [3]. The imagery map indicating the two sampled points with latitude 4°55'31.16"N, longitude 6°17'56.57"E, and latitude 4°55'30.77"N, longitude 6°17'56.83"E are shown in figure 1.

Fig. 1. Imagery map of the area under investigation showing the two sampled points

IV. Data Acquisition

The data acquisition started with identification of two survey points, where repeated profiles of thermal resistivity data were acquired. The process of data acquisition was carried out at each sampled point by excavating out the top soil majorly composed of humus organic material. The soil was dug up to a depth of 0.5 m with a shovel, followed by drilling of a hole of about 0.1 m deep. The probe made up of the thermocouple digital thermometer and heating element was inserted into the hole, and good contact between the hole and the probe was ensured. The current flowing in the circuit and voltage of the battery was measured and recorded with the help of the Digital Multimeter. The ambient temperature of the soil was recorded when the reading on the digital thermometer was steady. The circuit was completed by connecting the terminals of the heating element to the battery, at the same time the stop watch was started simultaneously. The readings on the digital thermometer after 0 s which is the ambient temperature of the soil, 5, 10, 15, 30, 45 and 60 s were noted and recorded; subsequently readings were taken every 30 s up to 35 minutes. Three independent thermal resistivity profiles data were acquired at each survey point, with an interval of 4 hours between each profile reading at each survey point.

V. Data Processing

The Data processing of thermal resistivity and conductivity started by entering the recorded data of temperature increase with time on a spread sheet, that was used to plot a graph of temperature in Kelvin versus time in seconds. The Measured voltage of the battery and the current flowing in the circuit were used to calculate the heat input, which in turn was used to calculate the thermal resistivity and thermal conductivity of the earth material making used of corresponding temperature values recorded between 720 s (12 minutes) and 2,100 s (35 minutes). The temperature recorded between these time interval falls within the steady state of the recorded thermal resistivity graph, which is generally known to be between 720 s (12 minutes) to 2700 s (45 minutes). The coordinates of the first slope that were used in determining the thermal resistivity of the soil material is between the temperature value recorded between 720 s (12 minutes) and 1560 s (26 minutes), after which, the slope coordinates were incremented to the next temperature and time value of 780 s (13 minutes) and 1620 s (27 minutes), to determine the next thermal resistivity value using the same heat input. A stepwise incremental process of thermal resistivity determination using the same heat input was continued until the coordinates of the final temperature recorded at 1260 s (21minutes) and 2,100 s (35 minutes) were used. The Stepwise generalized formulas for the modified computational approach to thermal resistivity determination are shown in equation 3 and 4. The average value of the determined thermal resistivity from the various slopes was found using equation 4, and these computed mean values were adopted as the true thermal resistivity of the soil material. The conventional thermal resistivity calculation as recommended by [6] and [2], usually carried out with just a single slope coordinate of say 12 minutes and 26 minutes, with their corresponding recorded temperature between these time intervals, was determined and noted for the purpose of comparison with the new modified computational method. Thermal conductivity was calculated by taking the inverse of the determined thermal resistivity. The results were subjected to statistical analysis to ascertain their level of accuracy and repeatability.

$$\sigma_i = \frac{4\pi}{Q}\left[\sum_{i<j}^{n} \frac{T_j - T_i}{ln\left(\frac{t_j}{t_i}\right)}\right] = \frac{4\pi}{Q}\left[\sigma_1 + \sigma_2 + \sigma_4 + \cdots \sigma_n\right] \quad (3)$$

Where

σ_i is total thermal resistivity (Km/W)

n is the upper limit

T_j is temperature at time t_j

T_i temperature at time t_i

Q is Heat input in (W/m)

$$\sigma_{average} = \frac{\sigma_i}{n} \qquad (4)$$

$\sigma_{average}$ is the true thermal resistivity of the soil material (Km/W).

VI. RESULTS AND DICUSSION

The outcome of the six thermal resistivity and conductivity data generated at the two survey points to ascertaining their repeatability and accuracy are shown in table 1 to 12 and Fig. 1 to 13. Both graphs of thermal resistivity and the semi log log graphs depict a general increase of temperature with time. Both graphs portray the initial heat up phase of the heating element and the steady state phase. Note that the acronym "TR" stand for Thermal Resistivity.

Table 1: Data Acquisition Parameters for Survey Point 1, TR1

Heat Input Parameters	Heat Input Parameters Values
Current (A)	0.1614
Resistance (Ohms)	73.3
Voltage (V)	12.47
Length of probe (m)	0.08
	Heat Input q (W/m)
Heat input Calc using Current and Resistance	23.86827585
Date	3/12/2019
Ambient Soil Temperature	300.2 K

Table 2: Measured temperature increase with time for Survey Point 1, TR1

S/N	Time (s)	Temperature K	S/N	Time (s)	Temperature K	S/N	Time (s)	Temperature K
1	0	300.2	28	660	302.5	54	1440	302.9
2	5	300.2	29	690	302.5	55	1470	302.9
3	10	300.2	30	720	302.5	56	1500	302.9
4	15	300.2	31	750	302.7	57	1530	302.9
5	30	300.5	32	780	302.7	58	1560	302.9
6	45	300.8	33	810	302.7	59	1590	302.9
7	60	300.8	34	840	302.7	60	1620	302.9
8	90	301.2	35	870	302.7	61	1650	302.9
9	120	301.5	36	900	302.8	62	1680	302.9
10	150	301.5	37	930	302.8	63	1710	302.9
11	180	301.8	38	960	302.8	64	1740	302.9
12	210	301.9	39	990	302.8	65	1770	302.9
13	240	301.9	40	1020	302.8	66	1800	302.9
14	270	302.1	41	1050	302.8	67	1830	302.9
15	300	302.1	42	1080	302.8	68	1860	302.9
16	330	302.1	43	1110	302.8	69	1890	303.0
17	360	302.2	44	1140	302.8	70	1920	303.0
18	390	302.2	45	1170	302.8	71	1950	303.0
19	420	302.3	46	1200	302.8	72	1980	303.0
20	450	302.3	47	1230	302.8	73	2010	303.0
21	480	302.3	48	1260	302.8	74	2040	303.0
23	510	302.3	49	1290	302.8	75	2070	303.0
24	540	302.5	50	1320	302.8	76	2100	303.0
25	570	302.5	51	1350	302.8	Improved Method 0.156498113 Km/W		
26	600	302.5	52	1380	302.9	Conventional Method 0.272481743 Km/W		
27	630	302.5	53	1410	302.9			

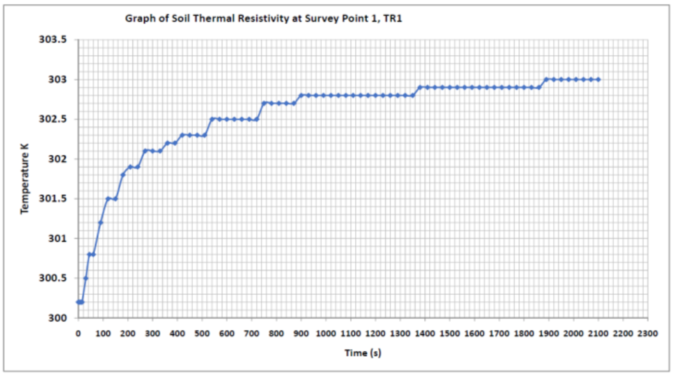

Fig. 2. Graph of Temperature in Kelvin (K) versus Time (s) at Survey Point 1, TR1

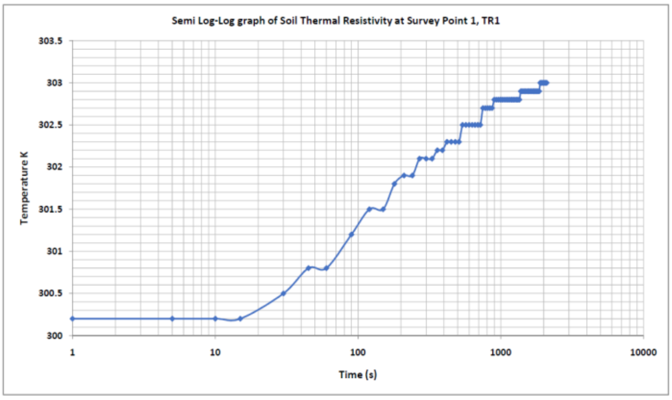

Fig. 3. Semi Log-Log graph of Measure Temperature increase with Time at Survey Point 1, TR1

Table 3: Data Acquisition Parameters for Survey Point 1, TR2

Heat Input Parameters	Heat Input Parameters Values
Current (A)	0.1635
Resistance (Ohms)	73.3
Voltage (V)	12.48
Length of probe (m)	0.08
	Heat Input q (W/m)
Heat input Calc using Current and Resistance	24.49342406
Date	3/12/2019
Ambient Soil Temperature	303.2

Table 4: Measured temperature increase with time for Survey Point 1, TR2

S/N	Time (s)	Temperature K	S/N	Time (s)	Temperature K	S/N	Time (s)	Temperature K
1	0	303.2	28	660	306.0	54	1440	306.2
2	5	303.2	29	690	306.0	55	1470	306.2
3	10	303.3	30	720	306.0	56	1500	306.2
4	15	303.4	31	750	306.0	57	1530	306.2
5	30	303.7	32	780	306.0	58	1560	306.3
6	45	304.1	33	810	306.0	59	1590	306.3
7	60	304.2	34	840	306.0	60	1620	306.3
8	90	304.5	35	870	306.1	61	1650	306.3
9	120	304.8	36	900	306.1	62	1680	306.3
10	150	305	37	930	306.1	63	1710	306.3
11	180	305.2	38	960	306.1	64	1740	306.3
12	210	305.2	39	990	306.1	65	1770	306.3
13	240	305.4	40	1020	306.1	66	1800	306.3
14	270	305.4	41	1050	306.1	67	1830	306.3
15	300	305.5	42	1080	306.1	68	1860	306.3
16	330	305.5	43	1110	306.2	69	1890	306.3
17	360	305.7	44	1140	306.2	70	1920	306.3
18	390	305.8	45	1170	306.2	71	1950	306.3
19	420	305.8	46	1200	306.2	72	1980	306.3
20	450	305.8	47	1230	306.2	73	2010	306.4
21	480	305.8	48	1260	306.2	74	2040	306.4
23	510	305.8	49	1290	306.2	75	2070	306.4
24	540	305.9	50	1320	306.2	76	2100	306.4
25	570	305.9	51	1350	306.2	Improved Method 0.175793698 Km/W		
26	600	305.9	52	1380	306.2	Conventional Method 0.199145373 Km/W		
27	630	306.0	53	1410	306.2			

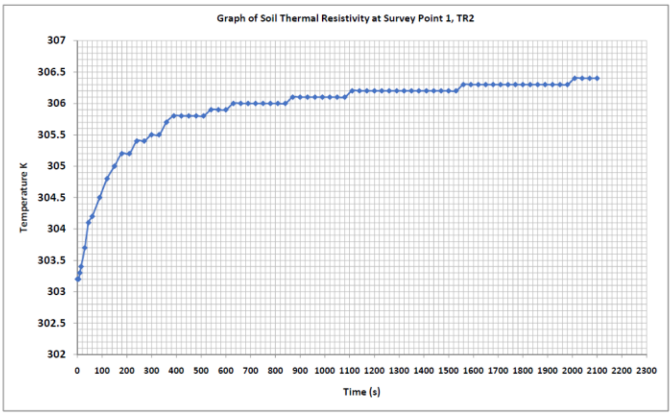

Fig. 4. Graph of Temperature in Kelvin (K) versus Time (s) at Survey Point 1, TR2

IJSES

International Journal of Scientific Engineering and Science
Volume 4, Issue 9, pp. 60-66, 2020.
ISSN (Online): 2456-7361

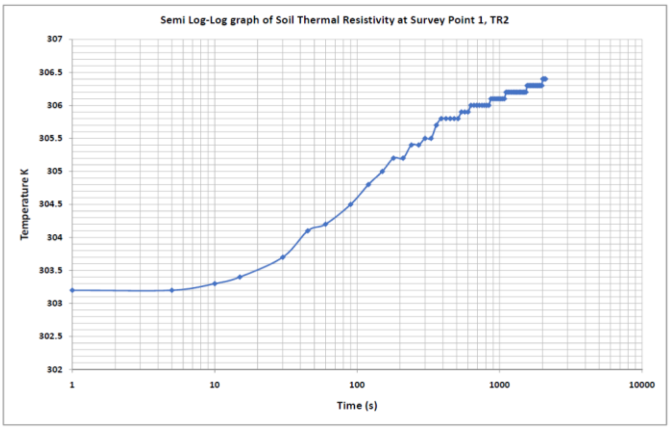

Fig. 5. Semi Log-Log graph of Measure Temperature increase with Time at Survey Point 1, TR2

Table 5: Data Acquisition Parameters for Survey Point 1, TR3

Heat Input Parameters	**Heat Input Parameters Values**
Current (A)	0.1608
Resistance (Ohms)	73.3
Voltage (V)	12.47
Length of probe (m)	0.08
	Heat Input q (W/m)
Heat input Calc using Current and Resistance	23.6911464
Date	3/12/2019
Ambient Soil Temperature	300.7

Table 6: Measured temperature increase with time for Survey Point 1, TR3

S/N	Time (s)	Temperature K	S/N	Time (s)	Temperature K	S/N	Time (s)	Temperature K
1	0	300.7	28	660	302.6	54	1440	302.9
2	5	300.7	29	690	302.6	55	1470	302.9
3	10	300.8	30	720	302.6	56	1500	302.9
4	15	300.8	31	750	302.6	57	1530	303.0
5	30	301.0	32	780	302.7	58	1560	303.0
6	45	301.2	33	810	302.7	59	1590	303.0
7	60	301.2	34	840	302.7	60	1620	303.0
8	90	301.4	35	870	302.8	61	1650	303.0
9	120	301.5	36	900	302.8	62	1680	303.0
10	150	301.7	37	930	302.8	63	1710	303.0
11	180	301.8	38	960	302.8	64	1740	303.0
12	210	302.0	39	990	302.8	65	1770	303.0
13	240	302.0	40	1020	302.8	66	1800	303.0
14	270	302.0	41	1050	302.9	67	1830	303.0
15	300	302.1	42	1080	302.9	68	1860	303.0
16	330	302.2	43	1110	302.9	69	1890	303.0
17	360	302.2	44	1140	302.9	70	1920	303.0
18	390	302.2	45	1170	302.9	71	1950	303.0
19	420	302.3	46	1200	302.9	72	1980	303.0
20	450	302.3	47	1230	302.9	73	2010	303.0
21	480	302.3	48	1260	302.9	74	2040	303.1
23	510	302.4	49	1290	302.9	75	2070	303.1
24	540	302.4	50	1320	302.9	76	2100	303.1
25	570	302.5	51	1350	302.9	Improved Method 0.174309062 Km/W		
26	600	302.5	52	1380	302.9	Conventional Method 0.274518983 Km/W		
27	630	302.5	53	1410	302.9			

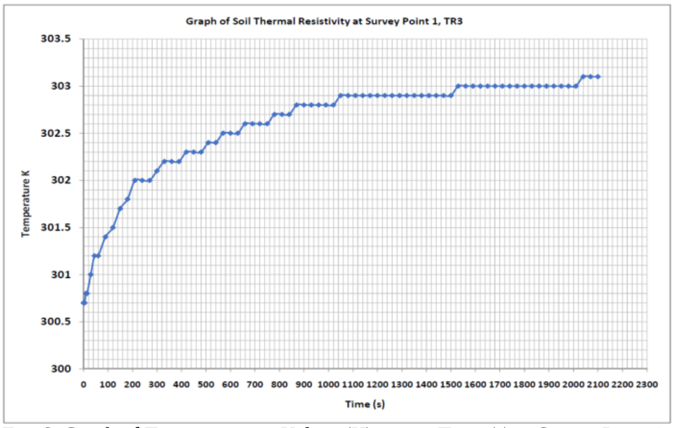

Fig. 6. Graph of Temperature in Kelvin (K) versus Time (s) at Survey Point 1, TR3

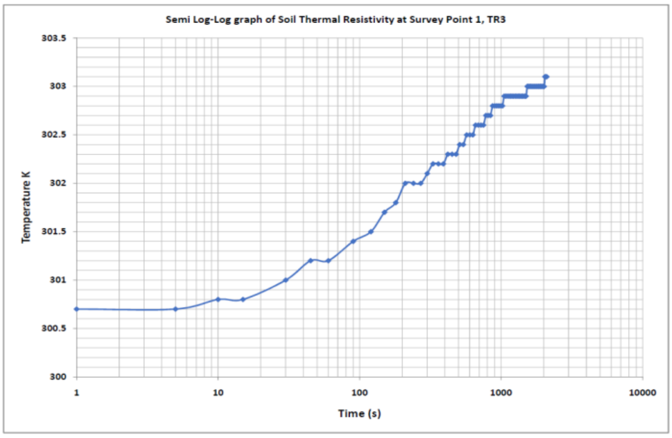

Fig. 7. Semi Log-Log graph of Measure Temperature increase with Time at Survey Point 1, TR3

Table 7: Data Acquisition Parameters for Survey Point 2, TR4

Heat Input Parameters	**Heat Input Parameters Values**
Current (A)	0.1604
Resistance (Ohms)	73.3
Voltage (V)	12.46
Length of probe (m)	0.08
	Heat Input q (W/m)
Heat input Calc using Current and Resistance	23.5734266
Date	4/12/2019
Ambient Soil Temperature	297.9

Table 8: Measured temperature increase with time for Survey Point 2, TR4

S/N	Time (s)	Temperature K	S/N	Time (s)	Temperature K	S/N	Time (s)	Temperature K
1	0	297.9	28	660	300.2	54	1440	300.7
2	5	297.9	29	690	300.2	55	1470	300.7
3	10	297.9	30	720	300.3	56	1500	300.7
4	15	298.1	31	750	300.3	57	1530	300.7
5	30	298.3	32	780	300.3	58	1560	300.7
6	45	298.3	33	810	300.3	59	1590	300.7
7	60	298.5	34	840	300.3	60	1620	300.8
8	90	298.9	35	870	300.3	61	1650	300.8
9	120	299.1	36	900	300.3	62	1680	300.8
10	150	299.2	37	930	300.3	63	1710	300.8
11	180	299.3	38	960	300.3	64	1740	300.8
12	210	299.4	39	990	300.5	65	1770	300.8
13	240	299.5	40	1020	300.5	66	1800	300.8
14	270	299.6	41	1050	300.5	67	1830	300.8
15	300	299.8	42	1080	300.5	68	1860	300.8
16	330	299.8	43	1110	300.5	69	1890	300.8
17	360	299.8	44	1140	300.5	70	1920	300.8
18	390	299.9	45	1170	300.5	71	1950	300.8
19	420	299.9	46	1200	300.5	72	1980	300.8
20	450	300.0	47	1230	300.5	73	2010	300.8
21	480	300.0	48	1260	300.5	74	2040	300.8
23	510	300.0	49	1290	300.5	75	2070	300.8
24	540	300.1	50	1320	300.5	76	2100	300.9
25	570	300.1	51	1350	300.7	Improved Method 0.331283852 Km/W		
26	600	300.1	52	1380	300.7	Conventional Method 0.275889862 Km/W		
27	630	300.2	53	1410	300.7			

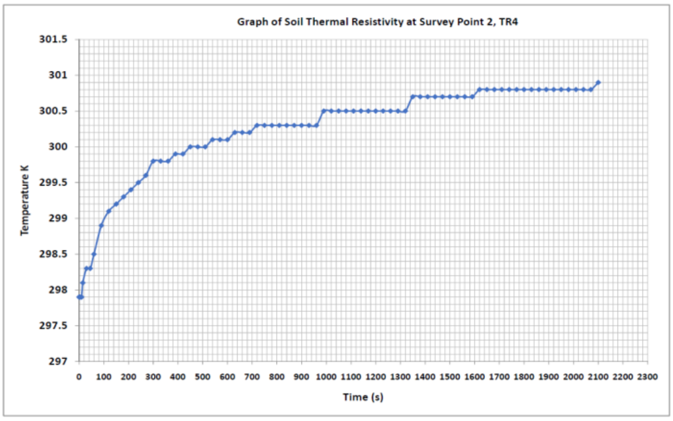

Fig. 8. Graph of Temperature in Kelvin (K) versus Time (s) at Survey Point 2, TR4

Volume 4, Issue 9, pp. 60-66, 2020.

International Journal of Scientific Engineering and Science
ISSN (Online): 2456-7361

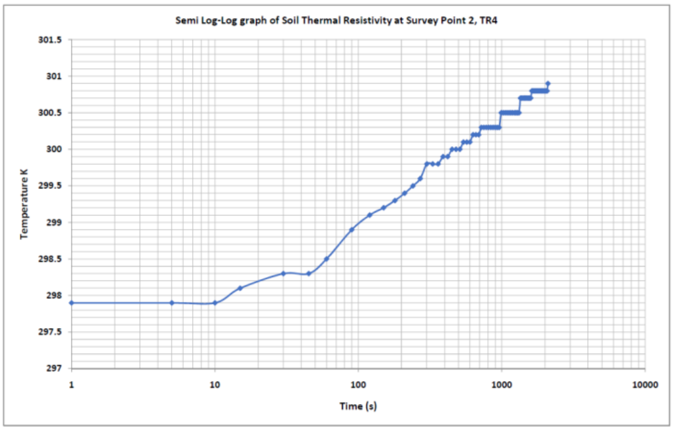

Fig. 9. Semi Log-Log graph of Measure Temperature increase with Time at Survey Point 2, TR4

Table 9: Data Acquisition Parameters for Survey Point 2, TR5

Heat Input Parameters	**Heat Input Parameters Values**
Current (A)	0.1608
Resistance (Ohms)	73.3
Voltage (V)	12.49
Length of probe (m)	0.08
	Heat Input q (W/m)
Heat input Calc using Current and Resistance	23.6911464
Date	4/12/2019
Ambient Soil Temperature	298.8

Table 10: Measured temperature increase with time for Survey Point 2, TR5

S/N	Time (s)	Temperature K	S/N	Time (s)	Temperature K	S/N	Time (s)	Temperature K
1	0	298.8	28	660	301.2	54	1440	301.6
2	5	298.8	29	690	301.2	55	1470	301.6
3	10	298.9	30	720	301.2	56	1500	301.6
4	15	298.9	31	750	301.2	57	1530	301.6
5	30	299.2	32	780	301.3	58	1560	301.8
6	45	299.5	33	810	301.3	59	1590	301.8
7	60	299.6	34	840	301.3	60	1620	301.8
8	90	299.9	35	870	301.4	61	1650	301.8
9	120	300.1	36	900	301.4	62	1680	301.8
10	150	300.2	37	930	301.4	63	1710	301.8
11	180	300.3	38	960	301.4	64	1740	301.8
12	210	300.5	39	990	301.4	65	1770	301.8
13	240	300.6	40	1020	301.4	66	1800	301.8
14	270	300.6	41	1050	301.5	67	1830	301.8
15	300	300.7	42	1080	301.5	68	1860	301.8
16	330	300.8	43	1110	301.5	69	1890	301.8
17	360	300.9	44	1140	301.5	70	1920	301.8
18	390	300.9	45	1170	301.5	71	1950	301.8
19	420	301.0	46	1200	301.5	72	1980	301.9
20	450	301.1	47	1230	301.5	73	2010	301.9
21	480	301.1	48	1260	301.6	74	2040	301.9
23	510	301.1	49	1290	301.6	75	2070	301.9
24	540	301.1	50	1320	301.6	76	2100	301.9
25	570	301.1	51	1350	301.6	Improved Method 0.351719346 Km/W		
26	600	301.1	52	1380	301.6	Conventional Method 0.411778474 Km/W		
27	630	301.1	53	1410	301.6			

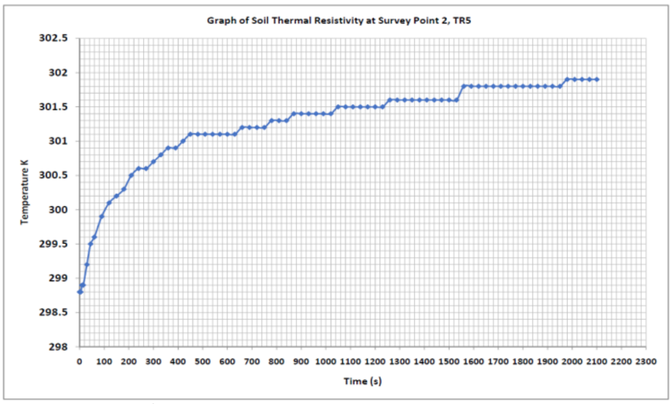

Fig. 10. Graph of Temperature in Kelvin (K) versus Time (s) at Survey Point 2, TR5

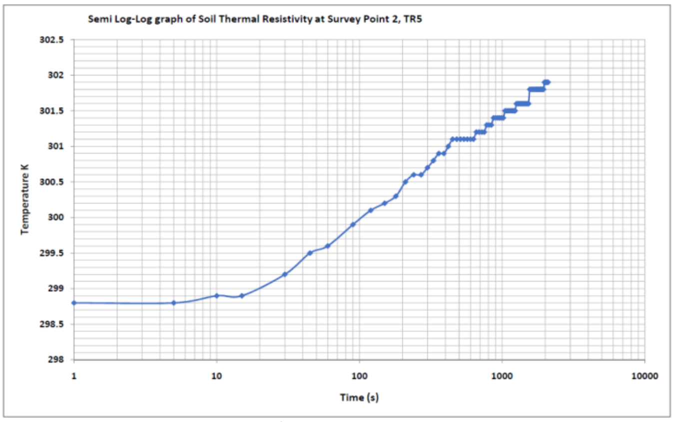

Fig. 11. Semi Log-Log graph of Measure Temperature increase with Time at Survey Point 2, TR5

Table 11: Data Acquisition Parameters for Survey Point 2, TR6

Heat Input Parameters	**Heat Input Parameters Values**
Current (A)	0.1629
Resistance (Ohms)	73.3
Voltage (V)	12.46
Length of probe (m)	0.08
	Heat Input q (W/m)
Heat input Calc using Current and Resistance	24.31398566
Date	4/12/2019
Ambient Soil Temperature	

Table 12: Measured temperature increase with time for Survey Point 2, TR6

S/N	Time (s)	Temperature K	S/N	Time (s)	Temperature K	S/N	Time (s)	Temperature K
1	0	298.9	28	660	301.2	54	1440	301.8
2	5	298.9	29	690	301.2	55	1470	301.8
3	10	298.9	30	720	301.3	56	1500	301.8
4	15	299.0	31	750	301.3	57	1530	301.8
5	30	299.3	32	780	301.3	58	1560	301.8
6	45	299.6	33	810	301.4	59	1590	301.8
7	60	299.8	34	840	301.4	60	1620	301.8
8	90	300.1	35	870	301.4	61	1650	301.8
9	120	300.3	36	900	301.4	62	1680	301.8
10	150	300.5	37	930	301.5	63	1710	301.8
11	180	300.5	38	960	301.5	64	1740	301.8
12	210	300.7	39	990	301.5	65	1770	301.8
13	240	300.7	40	1020	301.5	66	1800	301.8
14	270	300.8	41	1050	301.5	67	1830	301.9
15	300	300.8	42	1080	301.5	68	1860	301.9
16	330	300.9	43	1110	301.5	69	1890	301.9
17	360	300.9	44	1140	301.5	70	1920	301.9
18	390	300.9	45	1170	301.6	71	1950	301.9
19	420	301.1	46	1200	301.6	72	1980	301.9
20	450	301.1	47	1230	301.6	73	2010	301.9
21	480	301.1	48	1260	301.6	74	2040	301.9
23	510	301.1	49	1290	301.6	75	2070	301.9
24	540	301.1	50	1320	301.8	76	2100	301.9
25	570	301.2	51	1350	301.8	Improved Method 0.318063784 Km/W		
26	600	301.2	52	1380	301.8	Conventional Method 0.334358459 Km/W		
27	630	301.2	53	1410	301.8			

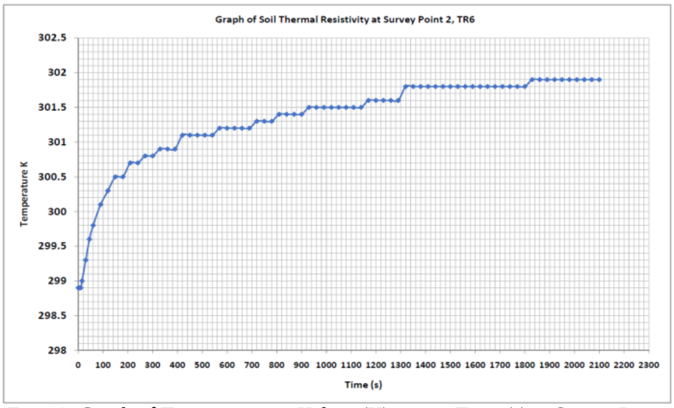

Fig. 12. Graph of Temperature in Kelvin (K) versus Time (s) at Survey Point 2, TR6

International Journal of Scientific Engineering and Science
Volume 4, Issue 9, pp. 60-66, 2020. ISSN (Online): 2456-7361

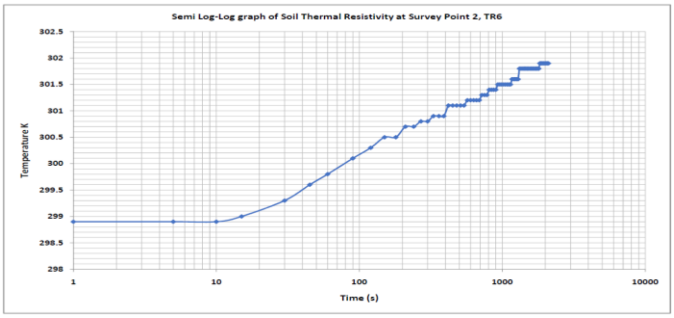

Fig. 13. Semi Log-Log graph of Measure Temperature increase with Time at Survey Point 2, TR6

The stepwise determined thermal resistivity values using the new modified computational approach for the two surveys points are shown in table 13. The range of thermal resistivity values determined at survey point 1 is between 0.079894397 Km/W to 0.282473725 Km/W, with a difference of 0.202579328 Km/W between these extreme values, and the range of thermal resistivity determined at survey point 2 is between 0.241027876 Km/W to 0.424181342 Km/W, with a difference of 0.183153466 Km/W. From the observed differences between range of the determined thermal resistivities values, if each value were to be independently adopted as the measured thermal resistivity value, using conventional method of a single slope approach, the result would have been grossly misleading. To get a pictorial view of this analogy, a graph of the determined stepwise thermal resistivity values was plotted against time. This graph also depicted the wide range and variation among thermal resistivity values determined at the same point and depth. The graph also revealed that, in most cases the graph start from a higher thermal resistivity value, goes down to a low thermal resistivity value, and then return back to a higher value.

The data in table 13 was subjected to simple statistical analysis by finding the average of all the stepwise determined thermal resistivity in each six columns in table 13 and also determining their standard deviation from the mean, of the resultant averages from each survey point (Table 14 to 16). Each of these average values represents the true values of thermal resistivities italicized and painted in green for survey point 1 and purple for survey point 2 in Table 13. This was compared with the first thermal resistivity values determined in each column of table 13, italicized and painted in red for survey point 1 and blue for survey point 2, which represent the data determined through conventional method that make use of a single slope.

The true thermal resistivities values and their final mean value, determined using modified computational approach in table 13 and 14 showed a high level of consistency and accuracy. The first two digits, by which most thermal resistivity values are reported, showed high level of repeatability at the two survey points. At survey point 1, the thermal resistivity values, registered a consistent value of 0.1 Km/W which is attributed to the thermal resistivity of sand rich in quartz present at that depth. At survey point 2, the true thermal resistivity registered a high consistence value of 0.3 Km/W, which could attributed to the presence of clay material at that depth. This goes a long way to justify the accuracy and high level of repeatability that could be achieved using modified computational approach. The thermal resistivity values determined through the conventional method making use of single slope (Table 13 and 14), registered a high level of disparity and inconsistency in values, that could not be tied to any lithological composition, or effectively used to classify the soil for thermal safety purpose. To confirm these results the standard deviation from the mean of the conventional method and modified computational approach were carried out as shown in table 15 and 16, and it was discovered for both thermal resistivity and conductivity that the standard deviation from the mean was least for the true thermal resistivities determined with modified computational approach, and highest for thermal resistivities values determined with the conventional method.

Table 13: The determined stepwise thermal resistivity (Km/W) values at the two survey points.

Front Stepwise Time (minutes)	Rear Stepwise Time (minutes)	Stepwise Thermal resistivity (Km/W) for Survey Point 1, TR1	Stepwise Thermal resistivity (Km/W) for Survey Point 1, TR2	Stepwise Thermal resistivity (Km/W) for Survey Point 1, TR3	Stepwise Thermal resistivity (Km/W) for Survey Point 2, TR4	Stepwise Thermal resistivity (Km/W)for Survey Point 2, TR5	Stepwise Thermal resistivity (Km/W)for Survey Point 2, TR6
12	26	*0.272481743*	*0.199145373*	*0.274518983*	*0.275889862*	*0.411778474*	*0.334358459*
12.5	26.5	0.140188726	0.204916012	0.282473725	0.283884328	0.423710588	0.344047171
13	27	0.144126234	0.210671528	0.217805715	0.364822304	0.363009525	0.353710491
13.5	27.5	0.148054265	0.216413190	0.223741813	0.374765206	0.372903021	0.290680440
14	28	0.151973588	0.222142126	0.229664753	0.384686070	0.382774589	0.298375394
14.5	28.5	0.155884893	0.151906227	0.157050384	0.394586635	0.314100768	0.306054605
15	29	0.079894397	0.155710489	0.160983473	0.404468461	0.321966946	0.313719279
15.5	29.5	0.081842922	0.159508074	0.164909660	0.414332943	0.329819319	0.241027876
16	30	0.083788270	0.163299467	0.168829445	0.424181342	0.337658889	0.246756937
16.5	30.5	0.085730666	0.167085106	0.172743281	0.260408877	0.345486562	0.336636405
17	31	0.087670313	0.170865388	0.176651579	0.266300599	0.353303157	0.344252766
17.5	31.5	0.179214791	0.174640673	0.090277355	0.272184533	0.270832065	0.351859060
18	32	0.183084166	0.178411289	0.092226507	0.278061190	0.276679522	0.359455947
18.5	32.5	0.186949056	0.091088768	0.094173400	0.283931037	0.282520201	0.367044030
19	33	0.190809743	0.092969843	0.096118177	0.289794500	0.384472706	0.374623860
19.5	33.5	0.194666485	0.189697992	0.098060965	0.295651971	0.392243860	0.286646958
20	34	0.198519517	0.193452683	0.200003770	0.301503809	0.400007541	0.292320560
20.5	34.5	0.202369059	0.197203972	0.203882093	0.307350344	0.407764187	0.297989021
21	35	0.206215310	0.200952055	0.207757101	0.417589177	0.311635652	0.303652637
Average of Stepwise thermal Resistivity, which represent the True Thermal Resistivity		*0.156498113 Km/W*	*0.175793698 Km/W*	*0.174309062 Km/W*	*0.331283852 Km/W*	*0.351719346 Km/W*	*0.318063784 Km/W*

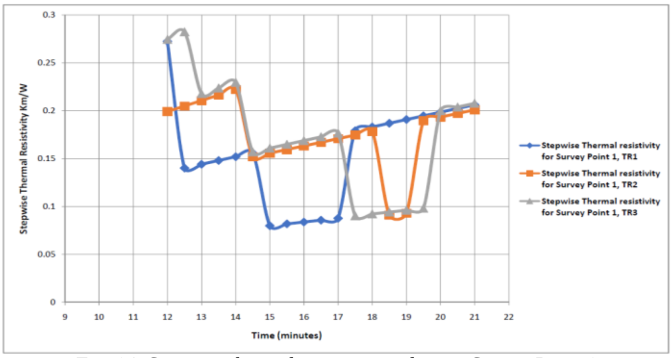

Fig. 14. Stepwise thermal resistivity values at Survey Point 1

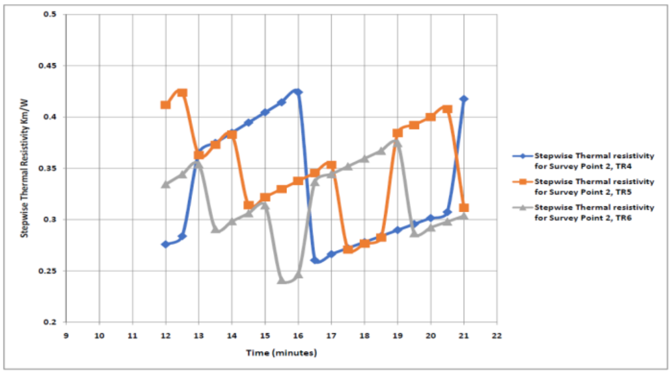

Fig. 13. Stepwise thermal resistivity values at Survey Point 2

Volume 4, Issue 9, pp. 60-66, 2020. *ISSN (Online): 2456-7361*

Table 14: Statistical analysis of the average values of conventional method and new computational Approach in thermal resistivity

	Thermal Resistivities determined with conventional method at survey point 1. Extracted from Table 13.	True Thermal Resistivities determined with new computational Approach at survey point 1. Extracted from Table 13.		Thermal Resistivities determined with conventional method at survey point 2. Extracted from Table 13.	True Thermal Resistivities determined with new computational Approach at survey point 2. Extracted from Table 13.
	0.272481743	0.156498113		0.275889862	0.331283852
	0.199145373	0.175793698		0.411778474	0.351719346
	0.274518983	0.174309062		0.334358459	0.318063784
Average	**0.248715366**	**0.168866958**	**Average**	**0.340675598**	**0.333688994**

Table 15: Statistical analysis of the Standard deviation from the mean for conventional method and new computational Approach in thermal resistivity

	Thermal Resistivities determined with conventional method at survey point 1.	True Thermal Resistivities determined with new computational Approach at survey point 1.		Thermal Resistivities determined with conventional method at survey point 2.	True Thermal Resistivities determined with new computational Approach at survey point 2.
	0.272481743	0.156498113		0.275889862	0.331283852
	0.199145373	0.175793698		0.411778474	0.351719346
	0.274518983	0.174309062		0.334358459	0.318063784
Standard deviation	**0.042940957**	**0.010737424**	**Standard deviation**	**0.068164202**	**0.016956201**

Table 16: Statistical analysis of the Standard deviation from the mean, for conventional method and new computational Approach in thermal conductivity

	Thermal Conductivities determined with conventional method at survey point 1.	Thermal Conductivities determined with new computational Approach at survey point 1.		Thermal Conductivities determined with conventional method at survey point 2.	Thermal Conductivities determined with new computational Approach at survey point 2.
	3.778667757	6.389853404		3.624634819	3.018559444
	5.021457365	5.688486057		2.428490227	2.843175991
	3.642735337	5.736936385		2.990802156	3.144023464
Standard deviation	**0.759811168**	**0.39169806**	**Standard deviation**	**0.598428558**	**0.151112419**

VII. CONCLUSION

The individual thermal resistivity and conductivity determined through the new modified computational stepwise techniques revealed a very wide range in thermal resistivity, that if any of these values were to be adopted as the actual thermal resistivity, as it is usually obtainable in conventional approach making use of single slope, the result could be very misleading. The final results has shown that the result obtained with modified computational approach showed high level of accuracy and consistency that could be tied to the existing lithological composition at both survey points. The thermal resistivity and conductivity determined through the conventional approach registered high level of disparity and inconsistency in values that are inaccurate and of very low repeatability that could not be tied to the existing lithology at that depth. This research work therefore has shown that the modified computational approach to thermal resistivity determination, is a more effective and accurate method than the conventional approach.

REFERENCES

[1] A. Kogbe, "The Cretaceous and Paleogene sediments of southern Nigeria". In: Geology of Nigeria, C.A. Kogbe, (editor), Elizabethan Press, Lagos: 311-334, 1989.

[2] ASTM (2000). Standard Test Method for Determination of Thermal Conductivity of Soil and Soft Rock by Thermal Needle Probe Procedure. Designation D 5334, Copyright © ASTM, 100 Barr Harbor Drive, West Conshohocken, PA 19428-2959, United States.

[3] C. C. Collins, "Evaluation of Natural Drainage Flow Pat-tern, Necessary for Flood Control, Using Digitized Topographic Information: A Case Study of Bayelsa State Nigeria". International Journal of Environmental, Ecological, Geological and Mining En-gineering. World Academy of Science, Engineering and Technol-ogy. http://www.waset.org/Publications Vol:8 No:7: 500-505, 2014.

[4] C. C. Collins, "Evaluation of Thermal Resistivity Response to Lithology, Gradational Soil Water Content and Ambient Soil Temperature". International Journal of Scientific Engineering and Science, Volume 4, Issue 5, pp. 55-63, 2020.

[5] C. C. Collins, "Impact of Soil Ambient Temperature on the Accuracy of Measured Thermal Resistivity". International Journal of Research, p-ISSN: 2348-6848, e-ISSN: 2348-795X Volume 06 Issue 12 November, 2019. http://edupediapublications.org/journals/index.php/IJR/

[6] IEEE Std. 442-1981 IEEE Guide for Soil Thermal Resistivity Measurements.

[7] J. B. Wright, D. A Hasting, W. B. Jones, and H. R.Williams, "Geology and mineral resources of West Africa", Allen and Unwin Limited, UK,: 107, 1985.

[8] K. C. Short, and A.J Stauble, "Outline of the geology of the Niger Delta". Bull. AAPG. 51: 761-779, 1967.

[9] M. A. Dafalla, "Improvement of Thermal Resistivity of Desert Sand for Use in High Voltage Cable Beddings and Foundation in Arid Zones". (2008).International Conference on Case Histories in Geotechnical Engineering. 28. https://scholarsmine.mst.edu/icchge/6icchge/session07/28

[10] M. A. Oladunjoye and O. A. Sanuade, "In Situ Determination of Thermal Resistivity of Soil: Case Study of Olorunsogo Power Plant, Southwestern Nigeria". International Scholarly Research Network, ISRN Civil Engineering Volume 2012, May 2012, Article ID 591450, 14 pages doi:10.5402/2012/591450

[11] M. U. Osakuni, and T. K. Abam, "Shallow resistivity measurement for cathodic protection of pipelines in the Niger Delta". Environmental Geology. 45: 2004, 747-752.

[12] S. C. Gaylon, and L. B. Keith, "The Effect of Soil Thermal Resistivity (RHO) on Underground Power Cable Installations", Printed in USA © 2014 Decagon Devices, Inc. 2014, www.decagon.com/thermal.